Parametrised Preisach Modelling of Hysteresis in High Temperature Superconductors

Mårten Sjöström, Dejan Djukic and Bertrand Dutoit

Swiss Federal Institute of Technology, Lausanne, Switzerland

Abstract

We present a parametrised Preisach-type model that describes the hysteresis exhibited by the high temperature superconductors (HTSC); hysteresis is the main cause for losses in the subcritical domain. The parametrised model, in combination with electrical measurements, is independent of geometry, number of filaments and other physical measures, and is identified by a novel method that uses electrical lock-in (loss) measurement technique, which greatly enhances the signal to noise ratio. Identification results from measurements on Bi-2223 multi-filamentary tapes are presented. We have further derived exact models for the hysteretic losses in strip and elliptic geometry strips, where the energy losses were calculated by Norris. The paper contains analysis of the Preisach model, of its losses and of the suggested parametrisation.

I. Introduction

HTSC is a new material with characteristics differing totally from conventional metallic conductors. The material is not fully free from losses, where the hysteretic losses are the main contribution at low-frequency (50-60 Hz) AC subcritical currents, subcritical temperatures and subcritical magnetic fields, see for instance [1].

It has been shown by Dejan Djukic [2]-[3] that the hysteresis in the HTSC tapes is conceptually similar to ferro-magnetic hysteresis and that it is therefore well described by the Preisach-type hysteresis model [7], concluded from the description of hysteresis in [8]. Arguments for the use of the Preisach model are also given in [9]-[10]. We have used the losses expressed by the Preisach model to derive exact models for the cases of strip and elliptic cross-section superconductors, whose losses were calculated by Norris [11]. All analytically known losses can also be used to calculate exact models by an expression given in the paper. The Preisach model further allows simulations of output voltage and losses for arbitrary input signals.

The model we propose in this paper is a parametrised Preisach model, which, in combination with electrical measurements, is independent of the many physical aspects of the HTSC tapes such as material, number of filaments, geometrical shape, coupling between filaments and so forth. Conventional first-transition curve identification (described in [9]) cannot be applied, so a novel method for the identification of the parameters from electrical lock-in (loss) measurements has been developed using sinusoids as input, however different from the identification method in [12]. The identification from losses is unique since Bean's model [13] implies an one-dimensional Preisach weighting function. The parametrisation further makes the model concise, accurate and quick in comparison with a memory consuming table look-up.

The standard electrical lock-in measuring technique greatly enhances the signal to noise ratio and is used to calculate the losses in the HTSC strip. These measured losses make the identification of the parametrised Preisach model possible. A parameter for a linear term in the model is used to comply it to the reactive part of the measurements. The paper presents the results of parametrisation and identification for measurements on Bi-2223 HTSC multi-filamentary tapes.

The paper begins by describing the hysteresis that is exhibited by HTSCs. The following section presents the Preisach model and why it is useful in this case. It also describes how losses can be

M. Sjöström, CIRC-EPFL, CH-1015 Lausanne, Switzerland, tel (+41-21) 693-5684, fax (+41-21) 693-6700, Marten.Sjostrom@epfl.ch, http://circwww.epfl.ch; D. Djukic, tel (+41-21) 693-2612, Dejan.Djukic@epfl.ch; B. Dutoit, tel (+41-21) 693-4689, Bertrand.Dutoit@epfl.ch

calculated and especially the special case of a sinusoidal input. It contains the exact models for strip and elliptic geometry tapes as well. The lock-in measurement techniques used for the identification part is described in the next section, which also explains how losses and reactive part can be extracted. We finally show how the parametrisation and identification are carried out by this measurement technique.

Part of the results for the parametrised Preisach model was firstly presented in [3], but are here given an improved and extended description.

II. Hysteresis in HTSCs

A. Hysteresis

The main source of the energetic losses in HTSC at low frequencies (up to 200 Hz), are the losses due to magnetisation hysteresis. In this section, we briefly discuss the hysteresis in HTSC.

All known HTSCs have physical properties of the superconductors of the type–II. Although the physical mechanisms related to the HTSC are not yet fully understood, some of their physical properties have been predicted, explained by theory and subsequently observed in measurements [4]–[6].

The main difference between the superconductors of the type–I and the type–II is their behaviour in presence of a magnetic field. This difference has its origins in the different ways the volume of a body with a non-zero demagnetising factor geometry is divided in domains in normal state and in superconducting state. In type–II superconductors, this division produces a mixed state: a state where the bulk of the body is in superconducting state which is transpierced by the flux tubes or vortices. The flux tubes are the domains in normal state which are in the form of microscopically thin threads or tubes. Each of the tubes carries a magnetic flux of exactly one fluxon ($\Phi_0 = \frac{h}{2e}$). The appearance of the flux tubes is observed macroscopically as the partial penetration of the flux into the volume of a superconducting body.

The imperfections of the crystal grid of the body have the property of attracting the flux vortices. The vortex which is attracted to a grid imperfection is held immobile by a force called the pinning force, and such a vortex is said to be pinned. The importance of the pinning forces is that the flux vortices remain immobile even under the influence of the Lorentz force, due to a magnetic field or a transport current. If the Lorentz force is weaker than the pinning force, the flux tube does not move, which means that no energy dissipation takes place. Hence, in the HTSC, the Meissner effect does not take place, yet the electrical resistance of such a body is zero for constant currents.

However, the pinning of the flux vortices means that the vortices that appear under the influence of a non-zero magnetic field will not disappear even if the field itself is removed. Since the body transpierced with flux vortices is macroscopically magnetised, the magnetisation of a HTSC shows hysteretic behaviour.

B. Model Limits

The hysteresis exhibited in HTSCs is present in the subcritical region and does not exist above the critical current according to the models in [8] and [13]. Therefore the hysteresis model is only valid for such currents. Physically, there is no abrupt limit but a gradual change from hysteretic losses to other sorts of losses. In fact, already at $0.8I_c$ flux creep losses start to appear for some samples [14], so that the pure hysteresis model is only valid up to such currents. Nevertheless, even if the physical grounds for the model is slightly violated, the parametrised Preisach model that we present in this paper is able to model losses up to the critical current. Allowing this extension makes it useful in a wider range. In the view of design purposes, it is also good that the model does not break down when it passes the limit of critical current, which is demonstrated in Section V.

III. The Preisach Model

Hysteresis can generally be described as a hysteresis transducer with an input signal $u(t)$ and an output signal $y(t)$. The Preisach model of hysteresis described here is slightly changed compared to

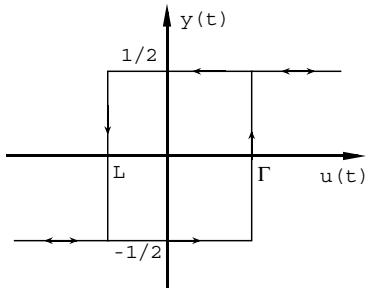

Fig. 1. The output due to the simplest hysteresis operator $\zeta_{\mathrm{L}\Gamma}$ is a rectangular loop in the output-input diagram which possesses an 'up'-switch at Γ and a 'down'-switch at L.

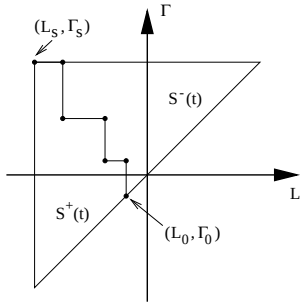

Fig. 2. Geometric interpretation of the Preisach model. The half-plane $\Gamma \geq \mathrm{L}$ is divided by $\mathcal{C}(t)$ into two parts where $\zeta_{\mathrm{L}\Gamma}$ is positive and negative respectively.

what can be found in the literature [9], but is conceptually the same. A more substantial description is given in [15].

The Preisach model consists of a superposition of an infinitely number of simplest hysteresis operator $\zeta_{\mathrm{L}\Gamma}$, each representing a rectangular loop in the output-input $(y-u)$ diagram, see Fig. 1. The output of the simplest hysteresis operator can take values $\pm 1/2$ only, where Γ and L correspond to the 'up' and 'down' switching, respectively. In the sequel, it is assumed that $\Gamma \geq \mathrm{L}$. Each $\zeta_{\mathrm{L}\Gamma}$ is weighted by an arbitrary weighting function $w(\mathrm{L},\Gamma)$, leading to the following expression for the output:

$$y(t) = \iint w(\mathrm{L},\Gamma)\zeta_{\mathrm{L}\Gamma}[u(t)]d\Gamma d\mathrm{L} \tag{1}$$

The Preisach model can be interpreted geometrically since there is a one-to-one correspondence between $\zeta_{\mathrm{L}\Gamma}$ and the point (L,Γ). There is a subdivision of the $\mathrm{L}-\Gamma$ plane into $S^+(t)$ and $S^-(t)$, the two parts where $\zeta_{\mathrm{L}\Gamma}$ is positive and negative respectively. This division depends on extrema of historic input and on the present input, and consists of a line of vertices $\mathcal{C}(t)$, see Fig. 2. The output of the hysteresis transducer then takes the following form:

$$y(t) = \frac{1}{2}\iint\limits_{S^+(t)} w(\mathrm{L},\Gamma)d\Gamma d\mathrm{L} - \frac{1}{2}\iint\limits_{S^-(t)} w(\mathrm{L},\Gamma)d\Gamma d\mathrm{L}\,. \tag{2}$$

since $\zeta_{\mathrm{L}\Gamma}[u(t)]$ is $\pm 1/2$ in $S^+(t)$ and $S^-(t)$. The erasing of extrema and the congruency of minor loops are the necessary and sufficient properties of a physical hysteresis to be described by the Preisach model, and the HTSC possesses these [10].

A HTSC has not got a saturation mode, but the weighting function $w(\mathrm{L},\Gamma)$ increases within the model limits, i.e. as long as the current in the HTSC is inferior to the critical current I_c (defined by the 1 μV/cm rule). The lack of saturation implies that the proposed estimation of $w(\mathrm{L},\Gamma)$ from

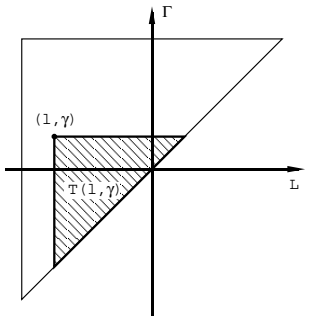

Fig. 3. The triangle that is limited by L=Γ and the coordinate (l, γ) as in the figure defines the surface over which the weighting function is integrated to form the function $W(l, \gamma)$.

first-order transition curves in [9] cannot be applied. Instead, we propose here estimations from lock-in measurements, described in Section V

Instead of the weighting function $w(\mathrm{L}, \Gamma)$, we can use the function $W(l, \gamma)$ which is the integral of $w(\mathrm{L}, \Gamma)$ over a triangular domain $T(l, \gamma)$ as the one presented in Fig. 3,

$$W(l, \gamma) \stackrel{\text{def}}{=} \iint\limits_{T(l,\gamma)} w(\mathrm{L}, \Gamma) d\Gamma d\mathrm{L} \,. \tag{3}$$

The weighting function $w(\mathrm{L}, \Gamma)$ can be extracted from $W(l, \gamma)$ by taking the derivative, first with respect to l and then with respect to γ in (3) when the input is increasing,

$$w(\mathrm{L}, \Gamma) = -\frac{\partial^2}{\partial \Gamma \partial \mathrm{L}} W(\mathrm{L}, \Gamma) \,, \tag{4}$$

and the reverse order of the derivatives when decreasing. There are certain advantages for the use of $W(l, \gamma)$, such as the calculation of double integrals is replaced by the calculation of finite sums [9],[15].

On physical grounds (symmetry considerations), it can be expected that the decreasing and increasing transition curves are congruent, which then has the consequence that

$$W(l, \gamma) = W(-\gamma, -l) \quad \text{and} \quad w(\mathrm{L}, \Gamma) = w(-\Gamma, -\mathrm{L}) \,. \tag{5}$$

The symmetry relation (5) is used to simplify expressions of the energetic losses, presented later in this section.

The Preisach model, as described above, is written in a general form and we continue in that way in the sequel, unless the model is specially applied, as in the HTSC case. In that case the output from the model, denoted by $y(t)$ above, corresponds to the flux

$$\Phi(t) = y(t) \tag{6}$$

that is induced by the input transfer current $i(t)$ in the superconductor. This transfer current $i(t)$ corresponds to the input denoted $u(t)$ in the general model above. Often the voltage $v(t)$ produced by the flux $\Phi(t)$ is measured instead of the flux itself, whereby the voltage is calculated as

$$v(t) = \frac{d\Phi(t)}{dt} = \frac{dy(t)}{dt} \,. \tag{7}$$

A. Energy Losses

It is well known that hysteresis phenomena are associated with some energy dissipation. Returning to the simplest hysteresis operator $\zeta_{\mathrm{L}\Gamma}$ and its representation in the output-input diagram (Fig. 1), it

is realised that the horizontal lines are reversible and hence give no energy loss. Therefore, the 'up' and 'down' switching contains all energy dissipation [9]. Symmetry considerations leads to assigning equal loss per switching,

$$q = \frac{1}{2}(\Gamma - \mathrm{L})\,. \tag{8}$$

The energy loss for any closed loop of a monotonically increasing and then monotonically decreasing input between the values u^- and u^+ has the following expression

$$Q_c(u^-, u^+) = \iint\limits_{T(u^-,u^+)} w(\mathrm{L},\Gamma)(\Gamma - \mathrm{L})d\Gamma d\mathrm{L}\,, \tag{9}$$

where $T(u^-, u^+)$ is the triangular surface in the $\mathrm{L}-\Gamma$ plane swept by the input signal during one cycle, c.f. Fig. 3. An inverse formula can be derived from (9) by which the weighting function $w(\mathrm{L},\Gamma)$ can be calculated from a known energy loss per cycle [2]:

$$w(\mathrm{L},\Gamma) = -\frac{1}{\Gamma - \mathrm{L}}\,\frac{\partial^2}{\partial \mathrm{L}\partial\Gamma}\,Q_c(\mathrm{L},\Gamma) \tag{10}$$

The formula (10) tells us that when the energy losses can be expressed analytically for a loop, the Preisach model can be derived with exact losses. The energy losses have been calculated for the cases of a sinusoidal transport current and superconductors with strip (index s) and with elliptical (index e) cross-sections by Norris [11]. The corresponding weighting functions $w(\mathrm{L},\Gamma)$ for these two cases then becomes [3]

$$w_s(\mathrm{L},\Gamma) = \frac{\mu_0}{4\pi I_c}\frac{x}{1-x^2}, \tag{11}$$

$$w_e(\mathrm{L},\Gamma) = \frac{\mu_0}{8\pi I_c}\frac{1}{1-x}, \tag{12}$$

$$\text{where} \quad x = \frac{\Gamma - \mathrm{L}}{2I_c}\,, \tag{13}$$

and μ_0 is the permeability in free space. Fig. 4 presents these one-dimensional weighting functions. The models can equally be described by the alternative weighting functions

$$W_s(\mathrm{L},\Gamma) = \frac{\mu_0 I_c}{2\pi}[(1-x)\ln(1-x) - (1+x)\ln(1+x) + 2x], \tag{14}$$

$$W_e(\mathrm{L},\Gamma) = \frac{\mu_0 I_c}{2\pi}[(1-x)\ln(1-x) + x], \tag{15}$$

The above weighting functions $w(\mathrm{L},\Gamma)$ and $W(l,\gamma)$ enable simulations of these two special cases.

The expression for the energy loss over a triangle $T(u^-, u^+)$ (9) can be re-written as a function of $W(l,\gamma)$ [9] and takes the following form:

$$Q_c(u^-, u^+) = (u^+ - u^-)W(u^-, u^+) - \int_{u^-}^{u^+} W(l, u^+)dl - \int_{u^-}^{u^+} W(u^-,\gamma)d\gamma\,. \tag{16}$$

In the case when the loop is between two input values that are symmetrically placed around zero, e.g. in the case of the sinusoidal input signal with peak value U_0,

$$u(t) = U_0\cos(\omega_0 t)\,, \tag{17}$$

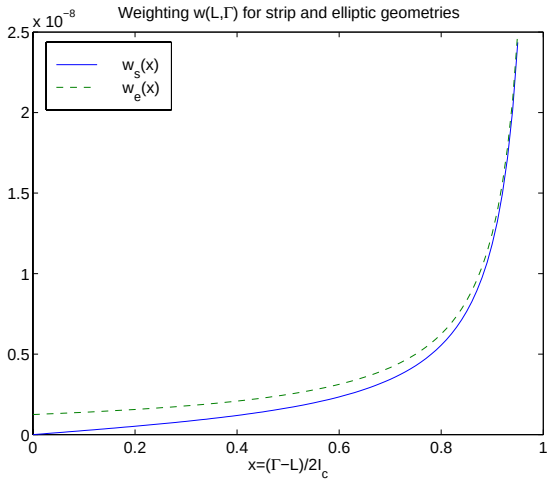

Fig. 4. Exact weighting functions for the cases of strip and elliptical cross section geometry superconductors. Solid and dotted lines correspond to (11) and (12), respectively

and symmetry (5) applies, the hysteretic losses of a full loop can be expressed by

$$Q_c(-U_0, U_0) = 2U_0 W(-U_0, U_0) - 2 \int_{-U_0}^{U_0} W(l, U_0) dl \,. \tag{18}$$

The above formula is useful when relating a parametrised $W(l, \gamma)$ and measured energy losses, so that the parameters can be identified as seen in Section V

IV. Measurements

The measurements are carried out on mono- and multifilamentary tapes at a temperature of 77 K where the injected sinusoidal current $i(t)$ and the voltage $v(t)$ induced by self-field are registered at a sample frequency of 10 kHz. The data are full of noise and their quality is enhanced by using the lock-in technique.

A. Lock-in Measurements

The lock-in technique enhances the quality of measurements and yields the in-phase and the quadrature signals so that the amplitudes for input and output (I_0 and V_0) and the phase-difference between the input and output ($\varphi_V - \varphi_I$) are retrieved for the input frequency ω_0 over the measured length l_t.

$$i(t) = I_0 \cos(\omega_0 t + \varphi_I) \tag{19}$$
$$v(t) = V_0 \cos(\omega_0 t + \varphi_V) \tag{20}$$

These measurements can be carried out for longer time intervals so that the in-phase and quadrature signals can be averaged. Hence, they yield results with a better quality.

The quantities retrieved by the lock-in technique enable us to calculate the power losses per cycle and unit length:

$$\hat{\hat{Q}}_c(-I_0, I_0) = \frac{\pi I_0 V_0}{\omega_0 l_t} \cos(\varphi_V - \varphi_I) \tag{21}$$

Note that the energetic losses are determined by the fundamental frequency of the output only, since the integration over a cycle for the higher harmonics gives zero.

The lock-in technique further allows us to retrieve the reactive amplitude, which is the part of the measured voltage $v(t)$ that has no contribution to the losses. Hence, it has an exact phase of $\pi/2$ after the input current, which can be expressed as

$$\hat{\hat{v}}_r(I_0) = \frac{V_0}{l_t}\sin(\varphi_V - \varphi_I)\,, \tag{22}$$

normalised with respect to the length over which the voltage measurement took place l_t. The above measure is used to adjust the suggested model to the reactive part of the measured voltage, see the following section.

V. Parametrisation and Identification

A. Parametrisation

We saw in Section III that it is better to use $W(l,\gamma)$ instead of $w(\mathrm{L},\Gamma)$ for implementation reasons. The integrated weighting function $W(l,\gamma)$ can easily include the modelling of a part that is reactive only, as will be clarified later in this section. Therefore, we will mainly be considering $W(l,\gamma)$.

The exact weighting functions for the cases of strip and elliptic cross-section superconductors given in (14) and (15) can also be expressed as Maclaurin-series of the variable $x = \frac{\Gamma-\mathrm{L}}{2I_c}$:

$$W_s(\mathrm{L},\Gamma) = \frac{\mu_0 I_c}{\pi}\sum_{k=1}^{\infty}\frac{x^{2k+1}}{(2k+1)2k} \tag{23}$$

$$W_e(\mathrm{L},\Gamma) = \frac{\mu_0 I_c}{2\pi}\sum_{k=1}^{\infty}\frac{x^{k+1}}{(k+1)k}\,. \tag{24}$$

It is clear that a subcritical input current,

$$i(t) = I_0\sin(\omega_0 t) \tag{25}$$

$$I_0 < I_c\,, \tag{26}$$

implies an x inferior to one, so that a truncation of the series gives small errors, especially far away from $x = 1$. Our approach to parametrise the weighting function then becomes

$$W(\mathrm{L},\Gamma,\theta) = I_c\sum_{k=1}^{K} a_k\Big(\frac{\Gamma-\mathrm{L}}{2I_c}\Big)^k\,, \tag{27}$$

where θ denotes the parameters gathered in a column vector,

$$\theta = [a_1, a_2, \ldots, a_K]^T\,. \tag{28}$$

It is also possible to select a parametrisation that uses every second term in (27), which reflects the sum in (23). We have, however, chosen to include all the terms since a parametrisation by every second term has not revealed any advantages in our investigations. Another issue is the choice of number of parameters, K. A large number assures that the true system can well be fitted in the model set, but on the other hand, a smaller K might be necessary to have statistical significance in the parameters. With a pragmatic approach, the agreement of simulated losses and measured data is of larger importance than the parameter variance. Note that K may also be bounded by the numerical stability of the estimation procedure.

For completion, we express the parametrised weighting function (27) in $w(\mathrm{L},\Gamma)$ by applying (4), which then takes the form

$$w(\mathrm{L},\Gamma,\theta) = \frac{a_1}{4I_c}\delta^+\Big(\frac{\Gamma-\mathrm{L}}{2I_c}\Big) + \frac{1}{4I_c}\sum_{k=2}^{K} a_k\,k(k-1)\Big(\frac{\Gamma-\mathrm{L}}{2I_c}\Big)^{k-2}\,. \tag{29}$$

where $\delta^+(x) \forall x \neq 0$ and $\int_0^\infty \delta^+(x)dx = 1$. Here, the Dirac function has been added so that this weighting function gives the same output as for (27). Below, we will derive how a_1 contributes to reactive power but not to hysteresis losses, which can be utilised for modelling of the reactive power in the measurements.

B. Model limits

The parametrised weighting function (27) is derived by assuming a subcritical input current (26) to avoid an infinite response of the weighting function. Now, having the parametrised version , that is no longer a necessity, since $W(\mathrm{L}, \Gamma, \theta)$ does not take infinite values for bounded L and Γ. Hence, the model does not beak down for currents superior to I_c, which is a desired behaviour.

C. Losses

Our approach is to estimate the parameters from loss measurements using the lock-in technique. Such an estimation also makes sense since a purpose with the model is to predict hysteretic losses. The lock-in technique gives better quality to the measurement results than time-series, and good estimates of the losses per cycle can, hence, be retrieved by applying (21). Noteworthy is that the suggested estimation method also give correct outputs as flux $\Phi(t)$ and voltage $v(t)$ (including reactive part, see sequel). The reason is that Bean's state model implies a weighting function that depends on the difference $(\Gamma - \mathrm{L})$, meaning a one-dimensional weighting function that is completely described by its parameters θ (and I_c).

Now we use the parametrisation in (27) to calculate the losses with the expression (18). This yields the following formula

$$Q_c(I_0, \theta_Q) = 2{I_c}^2 \sum_{k=1}^{K} a_k \frac{k-1}{k+1} \left(\frac{I_0}{I_c}\right)^{k+1} . \tag{30}$$

Note that the first parameter a_1 has no contribution to the losses, and therefore we exclude it from the parameter vector

$$\theta_Q = [a_2, \ldots, a_K]^T . \tag{31}$$

It is thus clear that a_1 cannot be identified from loss measurements. We remark that the parametrised expression for the losses (30) is linear in the parameters so that it can be written as a linear regression

$$Q_c(-I_0, I_0, \theta_Q) = \varphi^T(I_0)\, \theta_Q \tag{32}$$

with the regression vector

$$\varphi(I_0) = \left[\frac{1}{3}\left(\frac{I_0}{I_c}\right)^3, \frac{2}{4}\left(\frac{I_0}{I_c}\right)^4, \ldots, \frac{K-1}{K+1}\left(\frac{I_0}{I_c}\right)^{K+1} \right]^T . \tag{33}$$

Hence, we can estimate the parameters θ_Q as the Least Square Estimate (LSE) [16]:

$$\hat{\theta}_Q = \arg\min_{\theta_Q} \sum_{I_0} \alpha(I_0)\, (\hat{\hat{Q}}_c(I_0) - \varphi^T(I_0)\, \theta_Q)^2 \tag{34}$$

where we also include a possibility to put a weight $\alpha(I_0)$ to each measurement point.

The quality of the identification results depends on the number of parameters, K, and on the chosen weighting, $\alpha(I_0)$, where a bad choice can produce bizarre results such as simulated losses that are negative. To choose an appropriate model (K and $\alpha(I_0)$ in this case), it is important to remember the purpose of the model, including in what region of I_0/I_c we want to use it. When we simulate, we

TABLE I
ESTIMATED PARAMETERS FROM LOSS MEASUREMENTS AND THEIR CONFIDENCE INTERVALS

Param.	Estimated value	95% Confidence Interval		
$\hat{a}_2$	$-1.6093 \cdot 10^{-7}$	$-2.4517 \cdot 10^{-7}$	$\rightarrow$	$-7.6684 \cdot 10^{-8}$
$\hat{a}_3$	$1.8463 \cdot 10^{-6}$	$1.0994 \cdot 10^{-6}$	$\rightarrow$	$2.5931 \cdot 10^{-6}$
$\hat{a}_4$	$-8.4199 \cdot 10^{-6}$	$-1.1813 \cdot 10^{-5}$	$\rightarrow$	$-5.0268 \cdot 10^{-6}$
$\hat{a}_5$	$2.2484 \cdot 10^{-5}$	$1.3606 \cdot 10^{-5}$	$\rightarrow$	$3.1361 \cdot 10^{-5}$
$\hat{a}_6$	$-3.4628 \cdot 10^{-5}$	$-4.8558 \cdot 10^{-5}$	$\rightarrow$	$-2.0699 \cdot 10^{-5}$
$\hat{a}_7$	$2.9986 \cdot 10^{-5}$	$1.7035 \cdot 10^{-5}$	$\rightarrow$	$4.2937 \cdot 10^{-5}$
$\hat{a}_8$	$-1.3293 \cdot 10^{-5}$	$-1.9872 \cdot 10^{-5}$	$\rightarrow$	$-6.7151 \cdot 10^{-6}$
$\hat{a}_9$	$2.3420 \cdot 10^{-6}$	$9.3526 \cdot 10^{-7}$	$\rightarrow$	$3.7488 \cdot 10^{-6}$

Using loss measurements, the identified parameters $\hat{a}_k$ all have significant contribution to the parametrised model. The table contains the estimated values and the calculated 95 % confidence intervals in the case of $K = 9$. No confidence interval includes zero, so each parameter is significant for the model in this case.

would like indications on the hysteretic losses. It is therefore important with a good correspondence between modelled and measured losses in regions where losses are important, i.e. for large I_0. It is clear that the difference between modelled and measured losses

$$\varepsilon(I_0, \theta_Q) = \hat{\hat{Q}}_c(I_0) - \varphi^T(I_0)\,\theta_Q \tag{35}$$

grows quickly with input current I_0, meaning that larger I_0 naturally get more weight in the estimation procedure (34). To achieve a better model for small input currents, the extra weighting $\alpha(I_0)$ can be applied. Such a weight that increase the importance for smaller currents is chosen to be $(I_c/I_0)^2$, which corresponds to a weighting with the noise-to-signal ratio (NSR), approximately. [Note the contradiction to [3].]

A measure of the model goodness is the mean square error

$$\mathrm{MSE} = \frac{1}{N}\sum_{i=1}^{N} \varepsilon^2({I_0}^{(i)}, \theta_Q) \tag{36}$$

where N is the total number of data. However, this value always decreases with increasing number of parameters K. There exists a number of methods to choose a 'best' K in the sense that more parameters do not improve the model significantly for its purposes. Such methods, that introduces penalty terms for model complexity, are for instance Akaike's Information theoretic and final prediction-error criteria and Rissanen's minimum description length [16]. We have, however, chosen to formalise the selection of K by considering the parameter variances and carrying out standard statistical tests, or equivalently, computing confidence intervals [17]–[18], as well as a more pragmatic approach, where we have relied on visual inspection of convergence between graphs of measured and estimated losses.

To make the statistical tests, we compute the confidence interval for the estimated parameters. If it contains zero, we could consider to remove this parameter from the model, since it has no significance for the model. The 95% confidence interval for each of $\hat{a}_k$ is presented in Table I, with $K = 9$ and uniform weighting $\alpha(I_0) = 1$, showing that all $\hat{a}_k$ are significant. The simulated losses from the estimated weighting function $W(\mathrm{L}, \Gamma, \theta)$ has also a good agreement with the measured losses, except for small currents, see Fig. 5. The figure also shows that the losses coincide even better when $\alpha(I_0)$ is chosen to $(I_c/I_0)^2$ (NSR). The confidence in the parameters are then, however, reduced. With a pragmatic engineering approach, such a weighting function is nonetheless acceptable.

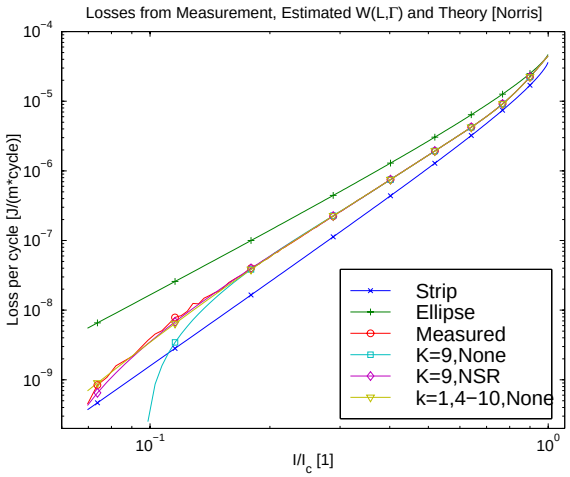

Fig. 5. Measured and estimated losses per cycle. Results depend on parametrisation (K=9) and if weighting (none or noise to signal ratio, NSR) is applied in the identification procedure. Good results are also retrieved by using parameters a_k, $k = 1, 4, 5 \ldots, 10$ with significance in the parameters.

Other choices of parameters are possible. For instance it is found, by removing parameters with large confidence intervals, that the use of the parameters a_k, $k = 1, 4, 5, \ldots, 10$ ($\alpha(I_0) = 1$) gives satisfactory results, see Fig. 5. Furthermore, the parameters are all statistically significant and the mean square error (36) is smaller than for $K = 9$.

D. Reactive part

We have just concluded that the parameters in the parametrised Preisach model can be identified from loss measurements with one exception, a_1, since it has no contribution to the losses. We show here how it contributes to the reactive part of the output voltage and it can, therefore, also be identified from lock-in measurements.

The technique to estimate the parameter a_1 from lock-in measurements is to consider the voltage contribution at a phase $\pi/2$ after the input current $i(t)$, which is calculated from the lock-in measurements according to (22). An expression for the same quantity using the Preisach model is retrieved by taking the derivative of the model output ($d\Phi(t)/dt$ in the HTSC case) when the increasing input current is equal to zero, since that corresponds to where the reactive voltage v_r has its maximum, see Fig. 6. That corresponds to an integration of $w(\mathrm{L}, \Gamma)$ over a small strip as in Fig. 7, or equally to the time derivative of $W(-I_0, i(t))$:

$$v_r(I_0) = \frac{d\Phi(t)}{dt}\Big|_{i(t)=0} = \frac{d}{dt} W(-I_0, i(t))\Big|_{i(t)=0} \tag{37}$$

The calculus when applied to the parametrised weighting function (27) leads to the following expression

$$v_r(I_0, \theta) = \frac{d}{dt} I_c \sum_{k=1}^{K} a_k \left(\frac{I_0 \sin(\omega_0 t) - (-I_0)}{2I_c} \right)^k \Big|_{t=0} \tag{38}$$

$$= \frac{\omega_0 I_0}{2} \sum_{k=1}^{K} a_k \, k \left(\frac{I_0}{2I_c} \right)^{k-1}, \tag{39}$$

and we realise that all the parameters θ contribute to the reactive amplitude. In principle, we could estimate all the parameters from (39), but since a correct hysteretic dissipation is desired, we insert

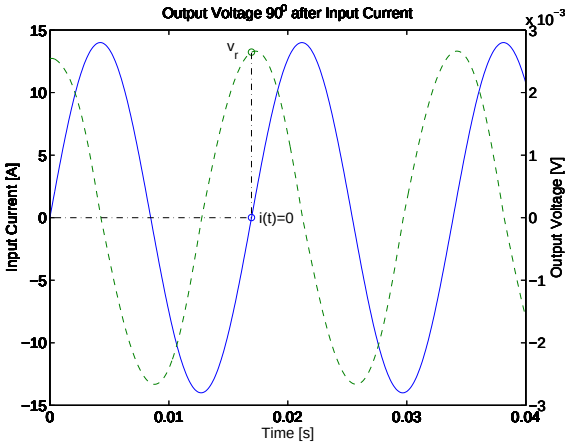

Fig. 6. The reactive part of the output voltage (dashed) is at a phase delay of $\pi/2$ after the input current (solid). The maximum of the reactive part is hence when the increasing current is zero.

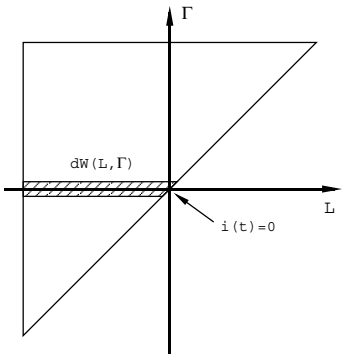

Fig. 7. The integration of the weighting function $w(\mathrm{L},\Gamma)$ over a small strip as in the figure corresponds to the maximum reactive part of the output voltage. By using the derivative of $W(-I_0, i(t))$ we include the parameter a_1.

the parameters θ_Q identified from losses and retrieve

$$v_{r-}(I_0,\theta_Q) = \left[v_r - \frac{\omega_0 I_0}{2}\sum_{k=2}^{K}\hat{a}_k\, k\left(\frac{I_0}{2I_c}\right)^{k-1}\right] = \frac{\omega_0 I_0}{2}\, a_1\,. \tag{40}$$

The formula (40) allows us to use the LSE technique to identify the parameter a_1,

$$\hat{a}_1 = \arg\min_{a_1}\sum_{I_0}\alpha(I_0)\,(\hat{\hat{v}}_{r-}(I_0) - \frac{\omega_0 I_0}{2}\, a_1)^2\,, \tag{41}$$

where $\hat{\hat{v}}_{r-}(I_0)$ is retrieved by replacing v_r by $\hat{\hat{v}}_r$ in (40). The confidence interval calculations can then be carried out, see Table II, where $\alpha(I_0)$ was taken to be uniform.

The estimated reactive amplitude, using the described method, coincides very well with measured $\hat{\hat{v}}_r$, as can be seen in Fig. 8, where the relative error is also shown. Note, that the graph of the reactive amplitude has a nonlinear shape. We conclude from the above discussion that a_1 can be used to conform the modelled output to have a correct reactive part.

VI. Conclusions

We have analysed the Preisach Model for hysteresis, which can be applied in regions of subcritical transport current, temperature and external magnetic field, where hysteresis contributes the most to

TABLE II
ESTIMATED a_1 FROM REACTIVE MEASUREMENTS AND ITS CONFIDENCE INTERVAL

Param.	Estimated value	95% Confidence Interval
$\hat{a}_1$	$1.1983 \cdot 10^{-6}$	$1.1853 \cdot 10^{-6} \rightarrow 1.2114 \cdot 10^{-6}$

The parameter $\hat{a}_1$ estimated from the reactive part of lock-in measurements has statistical significance, which is shown by the 95 % confidence interval in the table.

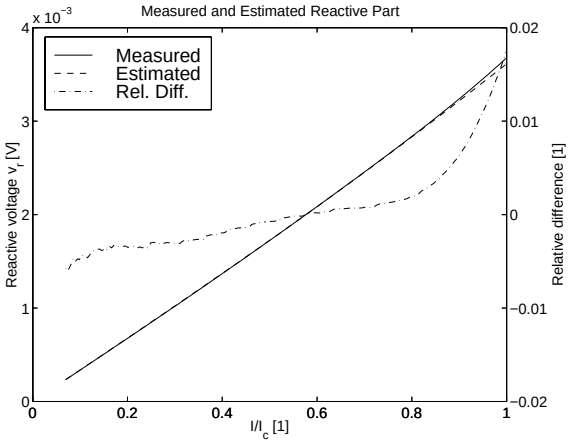

Fig. 8. The estimated reactive amplitude ($\pi/2$ after input current) (dashed in figure) fits very well with measured data (solid) when the parameter a_1 has been used to adjust the output, here with $K = 9$ and NSR weighting at estimation. Note that the graph is nonlinear c.f. (39). The relative error (dash-dotted, right scale) is below 1.8 % for this parametrisation.

dissipations in a HTSC tape. Exact models have been derived for the cases of strip and elliptic cross-section geometries. Furthermore, we have parametrised the model in such a way that it can easily be identified from high quality lock-in measurements, which makes the model independent of physical measures as geometry and number of filaments. The developed identification method ensures a correct modelling of losses in the HTSC and the parametrisation also allows for adjustments to the reactive part of the measured data.

REFERENCES

[1] T.Fukunaga, S. Maruyama, T. Abe and A. Oota, "AC Losses of Ag-Sheathed $(Bi,Pb)_2Sr_2Ca_2Cu_2O_x$ Superconducting Wires", *Physica C*, vol. 235-240, pp. 3231–3232, 1994.

[2] D. Djukic, "Modélisation des systèmes non-linéaires: ordre, adaptation des paramètres et hysterèse", *PhD thesis*, Chair of Circuit and Systems, Swiss Federal Institute of Technology, Lausanne, Switzerland, Nov. 1997.

[3] D. Djukic, M. Sjöström and B. Dutoit, "Preisach-type hysteresis modelling in Bi-2223 tapes", *Proc. 3rd European Conf. on Appl. Supercond.*, in press.

[4] A.C. Rose-Innes and E.H. Rhoderick, *Introduction to Superconductivity 2nd Ed.*. Oxford, England: Pergamon press, 1978.

[5] H.R. Ott, *Lecture Series on Superconductivity*. ETH, Zürich, Switzerland, 1996.

[6] M.V. Indenbom, A. Forkl, H.-U. Habermeier and H. Kronmüller, *J. Alloys Compounds.*, vol. 195 pp. 499, 1993.

[7] F. Preisach, *Z. Phys.*, pp. 277, 1935.

[8] E.H. Brandt and M. Indenbom, "Type-II-Superconductor Strip with Current in a Perpendicular Magnetic Field", *Phys. Rev. B*, vol. 48, pp. 12893–12906, 1993.

[9] I.D. Mayergoyz, *Mathematical Models of Hysteresis*. New York, USA: Springer Verlag, 1991.

[10] I.D. Mayergoyz, "Nonlinear Diffusion and Superconducting Hysteresis", *IEEE. Trans. on Magn.*, vol. 32, no. 5, pp. 4192–4197, 1996.

[11] W.T. Norris, "Calculation of hysteresis losses in hard superconductors carrying AC: isolated conductors and edges of thin sheets", *J. Phys. D: Appl. Phys.*, vol. 3, pp. 489–507, 1970.

[12] L. D'Alessandro and A. Ferrero, "A Method for the Determination of the Parameters of the Hysteresis Model of Magnetic Materials", *IEEE. Trans. on Instr. and Meas.*, vol. 43, no. 4, pp. 599–605, 1994.

[13] C.P. Bean, "Magnetization of High-Field Superconductors", *Rev. of Mod. Phys.*, vol. 36, pp. 31-39, 1964.

[14] S.P. Ashworth, "Measurements of AC losses due to transport currents in bismuth superconductors", *Physica. C*, vol. 229, pp. 355-260, 1994.
[15] M. Sjöström, "Preisach Modelling: Symmetry Implementation and Frequency Analysis", submitted to *IEEE. Trans. on Magn.*,
[16] L. Ljung, *System Identification – Theory for the User*. New Jersey, USA: Prentice-Hall Inc., 1987.
[17] A. Papoulis, *Probability, Random Variables and Stochastic Processes*. New York, USA: McGraw-Hill Inc., 1991.
[18] W.W. Hines and D.C. Montgomery, *Probability and Statistics in Engineering and Management Science*. 2nd Ed. New York, USA: John Wiley & Sons, 1980.